BMC Plant Biology

RESEARCH Open Access

The key metabolic pathway of roots and leaves responses in *Arachis hypogaea* under Al toxicity stress

Jianning Shi[1†], Yishuang Zhou[1†], Shaoxia Yang[1], Yingbin Xue[1], Yanyan Wang[1], Hanqiao Hu[1] and Ying Liu[1*]

Abstract

Background Aluminum (Al) toxicity inhibits plant growth and alters gene expression and metabolite profiles. However, the molecular mechanisms underlying the effects of Al toxicity on peanut plants remain unclear. Transcriptome and metabolome analyses were conducted to investigate the responses of peanut leaves and roots to Al toxicity.

Results Al toxicity significantly inhibited peanut growth, disrupted antioxidant enzyme systems in roots and leaves, and impaired nutrient absorption. Under Al toxicity stress, the content of indole-3-acetic acid-aspartate (IAA-Asp) decreased by 23.94% in leaves but increased by 12.91% in roots. Methyl jasmonate (MeJA) levels in leaves increased dramatically by 2642.86%. Methyl salicylate (MeSA) content in leaves and roots increased significantly by 140.00% and 472.22%, respectively. Conversely, isopentenyl adenosine (IPA) content decreased by 78.95% in leaves and 20.66% in roots. Transcriptome analysis identified 5831 differentially expressed genes (DEGs) in leaves and 6405 DEGs in roots, whereas metabolomics analysis revealed 210 differentially accumulated metabolites (DAMs) in leaves and 240 DAMs in roots. Under Al toxicity stress, both leaves and roots were significantly enriched in the "linoleic acid metabolism" pathway. Genes such as *lipoxygenase LOX1-5* and *LOX2S* were differentially expressed, and metabolites, including linoleic acid and its oxidized derivatives, were differentially accumulated, mitigating oxidative stress.

Conclusions This study elaborates on the potential complex physiological and molecular mechanisms of peanuts under aluminum toxicity stress, and highlights the importance of linoleic acid metabolism in coping with aluminum toxicity. These findings enhance our understanding of the impact of aluminum toxicity on peanut development and the response of key metabolic pathways, providing potential molecular targets for genetic engineering to improve crop resistance to aluminum stress.

Keywords *Arachis hypogaea*, Al toxicity stress, Transcriptomics, Metabolomics, Molecular mechanism

[†]Jianning Shi and Yishuang Zhou contributed equally to this work.

*Correspondence:
Ying Liu
liuying85168@gdou.edu.cn
[1]Department of Agronomy, College of Coastal Agricultural Sciences, Guangdong Ocean University, Zhanjiang 524088, China

Introduction

As human activities continue to intensify, the impact of acid deposition on the environment has become increasingly significant [1]. With rising soil acidity, more Al dissolves in the soil, making Al toxicity a key factor limiting plant growth in acidic soils [2].

Excessive accumulation of aluminum (Al) can increase reactive oxygen species (ROS) in plants. This leads to lipid peroxidation and dysfunction of plasma membrane organelles [3]. Al toxicity primarily affects the root system of plants [4]. Al binds to unmethylated pectin in cell walls, causing significant accumulation in the roots. This accumulation can increase the rigidity of the cell wall and reduce its ductility [5]. Al also disrupts the cytoskeletal system through calcium signaling. This leads to the deaggregation of microtubules and microfilaments, as well as chromosome adhesion and spindle filament destruction. Such changes inhibit cell division and can result in the enlargement of root tips in plants [6]. These effects negatively impact root growth and nutrient uptake. For instance, in Al-sensitive Eucalyptus clones (*Eucalyptus grandis* × *Eucalyptus urophylla* G4), Al toxicity leads to root tip expansion and a significant decrease in nitrogen (N) and potassium (K) content in the root system [4]. The adverse effects of Al stress extend to plant leaves, primarily manifesting as reduced chlorophyll content, diminished photosynthetic capacity, and lower nutrient levels [7]. Moreover, Al stress disrupts the photosystem and decreases pigment content, resulting in lower photosynthetic efficiency (De Sousa et al., 2022). For example, Al-sensitive rye (*Secale cereale*) exhibits enlarged chloroplasts and increased Al accumulation under Al stress, leading to reduced chlorophyll content and impaired photosynthesis [8]. In crops like maize (*Zea mays*), sorghum (*Sorghum bicolor*), and other Al-sensitive species, even low concentrations of Al can inhibit leaf elongation and negatively affect photosynthetic capacity [9, 10].

The physiological response mechanisms of plants to Al toxicity stress are complex and varied. These mechanisms include the secretion of organic acids and mucus by roots, the elevation of rhizosphere pH, the fixation of Al on cell walls, the compartmentalization of Al in vacuoles, and the chelation of Al by intracellular organic acids [11]. Plant responses to Al toxicity stress can be categorized into two types: internal tolerance mechanisms and external rejection mechanisms, based on whether they occur inside or outside the plant cells [12]. Studies on external rejection mechanisms indicate that root tips secrete organic acids, such as citric acid, oxalic acid, or malic acid. These organic acids chelate Al in the rhizosphere, preventing its entry into root cells [13]. Research on internal tolerance mechanisms reveals that root cell walls are rich in carboxyl substances, including pectin, cellulose, and hemicellulose. These substances have a high affinity for Al, facilitating its fixation in the cell wall [14, 15]. Additionally, evidence suggests that internal detoxification of Al involves chelation of intracellular Al and compartmentalization of Al-organic acid complexes into vacuoles [12]. Although current research primarily focuses on traditional physiological characteristics of plant responses to Al toxicity stress, the molecular regulatory mechanisms involved remain unclear. Understanding these molecular mechanisms will enhance our ability to improve crop resistance to Al and identify high-quality varieties with Al resistance.

Plant hormones can regulate plant growth and help plants adapt to external stresses [16]. For instance, the application of cytokinins intensifies the undulation of lettuce (*Lactuca sativa*) leaves [17]. After cucumber (*Cucumis sativus*) is subjected to salt stress, the application of exogenous salicylic acid (SA) can help improve photosynthesis in the leaves, thereby alleviating salt stress [18]. In blueberries (*Vaccinium corymbosum*), the application of exogenous methyl jasmonate (MeJA) can mitigate the damage caused by Al toxicity stress [19].

In recent years, the advancement of omics technologies, including transcriptome sequencing (RNA-seq) and metabolomics, along with multi-omics combined analysis, has provided a comprehensive perspective on plant responses to stress [20]. Transcriptomics via RNA-seq and metabolomics, which reveal changes in metabolite levels, have been instrumental in studying plant responses to Al toxicity. This offers a new lens through which to understand Al toxicity stress in plants [21–23]. Research indicates that increasing the pH in the culture environment can mitigate the effects of Al poisoning on gene expression in sweet orange (*Citrus sinensis*) leaves, enhancing the adaptability of metabolites to Al stress [21]. Combined transcriptomic and metabolomic analyses of sweet orange leaves show that various metabolic pathways, such as glycolysis/gluconeogenesis and phenylpropanoid pathways, along with metabolites like callosal and phenolic compounds, and genes including *XTHs*, *PAPs*, *PCS3*, and *CS*, may play a role in alleviating leaf Al toxicity when pH is elevated [21]. In a separate study, transcriptomic and metabolomic analyses of rice roots (*Oryza sativa*) explored the molecular differences in Al stress resistance among rice varieties from two locations. The findings suggest that phenylpropanoid biosynthesis is a critical pathway in rice roots' response to Al toxicity [22]. Another investigation identified key candidate genes related to Al tolerance in rape (*Brassica napus*). Using root quantitative trait genes (QTGs), differentially expressed genes (DEGs), and differentially accumulated metabolites (DAMs) data from Al-resistant and Al-sensitive rape under Al toxicity stress, this study found that these genes primarily participate in lipid, carbohydrate, and secondary metabolite metabolism [23].

Peanut (*Arachis hypogaea*) is a significant source of fat and protein. Its production development has been crucial for increasing oil and protein supply, thus enhancing the agricultural production cycle [24]. By 2021, China's peanut cultivation area reached 4.73 million hectares, yielding 17.99 million tons. This growth has notably contributed to China's oil production, ensuring a stable supply of vegetable oil and reducing reliance on imports [25]. However, studies indicate that Al toxicity negatively impacts peanut growth in acidic environments [26]. Currently, the molecular regulatory mechanisms of peanuts in response to Al toxicity remain unclear. Utilizing multi-omics approaches may help identify key genes and mechanisms involved in this stress response. This study aims to investigate the molecular responses of peanut leaves and roots to Al toxicity, laying the groundwork for developing new Al-resistant peanut varieties.

Materials and methods

Plant materials and treatment methods

The peanut variety used in this experiment was Zhanyou 62, developed by the Zhanjiang Institute of Agricultural Sciences in Guangdong Province. The plants were cultivated in the experimental field of Guangdong Ocean University (E: 110.30311, N: 21.15005). Full-sized peanut seeds of similar size were selected and sterilized with 1% NaClO (Guangzhou Reagent, Guangzhou, China) for 10 min. After sterilization, the seeds were placed in sterilized white quartz sand for 10 days. Consistently growing seedlings were then selected and transplanted into 15 L blue plastic boxes, where nutrient solution was added for hydroponics [27]. The nutrient composition of the hydroponic solution is detailed in Table S1.

All chemical reagents used in Table S1 were analytically pure grade reagents (Kermel, Tianjin, China). $Al_2(SO_4)_3{\cdot}18H_2O$ (Hushi, Shanghai, China) served as the Al source. The nutrient solution for treatment included control (0 mM) and 0.4, 1.2, 4, and 10 mM Al concentrations. The pH of the hydroponic nutrient solution was adjusted to approximately 4.0 using 1 M hydrochloric acid (Guangzhou Reagent, Guangzhou, China) [28]. Each treatment concentration was repeated three times, with a total of 30–36 peanut seedlings per concentration. The plant culture room was maintained at 25–30 ℃ during the day and 18–22 ℃ at night to ensure optimal plant development. The photoperiod lasted about 12 h per day, with a light intensity of 2000 lx. The nutrient solution was changed every 5–6 days. After 20 days of Al treatment, peanut leaves (the fourth leaf from the bottom) and roots were collected for further testing.

Measurement of four physiological indexes

To assess phenylalanine ammonia lyase (PAL) activity, total antioxidant capacity (T-AOC), reduced glutathione (GSH) content, and hydrogen peroxide (H_2O_2) content in peanut leaves and roots subjected to different Al treatment concentrations (0, 0.4, 1.2, 4, and 10 mM) for 20 days, samples of 0.10 g were rapidly frozen in liquid nitrogen and ground into a fine powder. These parameters were measured using detection kits (Boxbio Co., Ltd, Beijing, China) in accordance with the manufacturer's instructions, with three biological replicates for each treatment.

Measurement of biomass-related indicators and microscopic observation

The above-ground and root fresh weight of each peanut plant was measured using an BS124S electronic balance (Sartorius, Göttingen, Germany).

A WinRHIZO LA6400 XL root scanner (Regent, Vancouver, BC, Canada) was used to scan the morphological indices of the peanut roots and capture images of each treated peanut root system. WinRHIZO software (WinRHIZO 2013e Professional Edition) was subsequently used to analyze and obtain data concerning the surface area, volume, total length, and number of roots. Three measurements were obtained for each treatment.

Peanut taproot tips, treated with 0 mM and 4 mM Al for 20 days, were carefully collected. Following freeze-drying, samples were fixed on a test stand and examined using a Regulus 8100 scanning electron microscope (Hitachi, Tokyo, Japan), with three biological replicates for each treatment [4].

Determination of the content of four elements

Determination of Al, P and B elements

Leaves and roots from peanut seedlings treated with 0 and 4 mM Al for 20 days were collected as samples. The samples were baked in a constant temperature drying oven (Yiheng, Shanghai, China) at 60 °C for 7 days. After baking, the samples were weighed to approximately 0.15 g and dissolved completely in nitric acid (Huada Corporation, Guangzhou, China). The samples were then transferred into a tetrafluoroethylene crucible (30 mL) (Puqi, Yancheng, China), and 5 mL of 98% concentrated nitric acid (Huada Corporation, Guangzhou, China) was added. The mixture was allowed to stand for 24 h. Next, the crucible was placed on a heating plate (Richen LC-DB-3EFS, Shanghai, China), where the temperature was gradually raised to 180 °C for digestion over 2 to 3 h. Following this, 2 mL of nitric acid (68%) and 2 mL of H_2O_2 (30%) (Guangzhou Reagent, Guangzhou, China) were added to the crucible and digested on the electric heating plate at 180 °C for an additional 3 to 5 h. After cooling to room temperature, 1 mL of nitric acid (68%) was added to leach the sample. All extracts and residues were then transferred to a 25 mL colorimetric tube (Zhihong, Taizhou, China) containing deionized water. The

contents of Al, P (Phosphorus), and B (Boron) in the peanut leaves and roots were determined using ICP-MS (NexION®1000 ICP-MS, PerkinElmer, Massachusetts, USA) [29, 30]. Each Al treatment concentration was repeated three times.

Determination of N element content

Samples of leaves and roots from peanut seedlings treated with 0 and 4 mM Al for 20 days were collected. The total N content in these samples was determined using a published method [31]. Approximately 0.2 g of plant material (dry weight) was dissolved in 98% H_2SO_4 (Guangzhou Reagent, Guangzhou, China). The N content in the peanut leaves and roots was measured using an automatic Kjeldahl nitrogen analyzer (FOSS Kjelte 8400, Denmark, Europe).

Determination of four hormone contents

Leaves (fourth leaf position) and root systems treated with 0 and 4 mM Al^{3+} for 20 days were used as samples. High-performance liquid chromatography-tandem mass spectrometry (HPLC-MS/MS) (PE QSight 420, PerkinElmer, Massachusetts, USA) was employed to extract endogenous plant hormones and determine their contents in peanut samples. The hormones analyzed included IAA-ASP, MEJA, MESA, and IPA, with internal standards added to the extraction solution to correct the detection results [32]. The external standards used for analysis, such as IAA-ASP, MEJA, MESA, and IPA, were pure chromatographic reagents purchased from Sigma (Saint Louis, MI, USA). The internal labels used were deuterated versions of IAA (D-IAA), JA (D-JA), SA (D-SA), and Zeatin (D-Zeatin) from Sigma. The chromatographic column was packed with C18 QuEChERS (Shanghai Amperex, Shanghai, China), and the solvents used were chromatography-grade methanol and acetonitrile (Merck, Darmstadt, Germany).

Liu et al. [33] studied the preparation of the working solution, the calculation of the hormone content standard curve, and the extraction of hormones from peanut leaves. Additional information, including HPLC gradient parameters, mass spectrometry parameters, and the selected monitoring conditions for protonated or deprotonated plant hormone reactions, can be found in Supplementary Table S2.

cDNA library preparation and transcriptome sequencing analysis

Leaves and roots (0.10 g per sample) were collected from peanut seedlings treated with 0 mM and 4 mM Al. Each treatment included three biological replicates. The samples were ground in liquid nitrogen, and DNA libraries were constructed following the method outlined by Liu et al. [33]. These libraries were sequenced using Illumina sequencers. The raw sequencing data was filtered to produce clean data for high-quality analysis. The clean data were then aligned to the peanut reference genome of Peanut Base (https://www.peanutbase.org/) (arahy.Tifrunner.gnm2.J5K5.genome_main.fna) using Tophat software (Version 2.1.1). To analyze gene expression levels, HTSeq software (Version 0.9.1) was utilized to count the read values for each gene, which were then considered as the original expression amounts. DESeq software (Version 1.20.0) was employed for differential analysis of gene expression. DEGs were identified using the following criteria:|log2FoldChange| > 1 and a significant P-value < 0.05. Kyoto Encyclopedia of Genes and Genomes (KEGG) pathway enrichment analysis was conducted using clusterProfiler (Version 3.4.4). These data were submitted to the NCBI database under registration number PRJNA1175555 (https://www.ncbi.nlm.nih.gov/bioproject/PRJNA1175555).

Metabolome analysis

Leaves and roots (0.10 g per sample) were obtained from peanut seedlings treated with 0 mM and 4 mM Al, with four biological replicates for each treatment. Sample preparation and data analysis for metabolomics were conducted using standard procedures from Suzhou Panomic Biomedical Technology Co., China. Detected metabolites were analyzed using Liquid chromatography tandem mass spectrometry (LC-MS/MS), specifically the Thermo Vanquish ultra-high-performance liquid phase system (Thermo Fisher Scientific, USA) and the Thermo Orbitrap Exploris 120 mass spectrometry detector (Thermo Fisher Scientific, USA). Quantitative results were derived using methods reported by Rasmussen et al. [34] and Navarro-Reig et al. [35]. Principal component analysis and Orthogonal partial least squares discriminant analysis (OPLS-DA) were performed for data reduction and regression. Qualitative results were obtained by referencing spectral databases, including HMDB, Massbank, LipidMaps, Mzcloud, KEGG, and Nomi Metabolism. Secondary identified metabolites were selected based on a P-value < 0.05 and VIP > 1 to identify DAMs [36]. These DAMs were then used for KEGG pathway enrichment and co-analysis with transcriptome data.

Fluorescence quantitative RT-PCR (qRT-PCR) analysis

Peanut leaves and roots treated with 0 mM and 4 mM Al for 20 days were collected as samples. RNA was extracted using the MolPure Plant RNA Kit (Yeasen, China). cDNA was synthesized through reverse transcription of the RNA with the Hifair II 1st Strand cDNA Synthesis Kit (Yeasen, China). The Hifair UNICON Universal Blue qPCR SYBR Green Master Mix (Yeasen, China) was employed alongside the ABI7500 fluorescence quantitative PCR (Applied Biosystems, USA) to assess target gene

expression [37]. qRT-PCR was performed to analyze the expression of key responsive pathway-related genes in peanut leaves and roots. We utilized a 20 μL qRT-PCR system, which included 0.5 μL of the upstream primer, 0.5 μL of the downstream primer, 8 μL of nuclease-free water, 1 μL of the cDNA template, and 10 μL of the Hifair UNICON Universal Blue qPCR SYBR Green Master Mix (Yeasen, China). The qRT-PCR cycle conditions were set as follows: 95 ℃ for 10 min; 95 ℃ for 15 s; 60 ℃ for 1 min; repeated for a total of 40 cycles [38]. Serial dilutions of the reverse-transcribed peanut cDNA template were prepared as standards: the original cDNA was designated as Standard 1, followed by a five-fold dilution of Standard 1 to generate Standard 2. This dilution method was repeated sequentially to produce Standards 3, 4, and 5 for standard curve construction. The gene *AhUbiquitin* (*DQ887087.1*) was chosen as the internal reference gene, and the relative gene expression level was calculated as the target gene expression level divided by the internal reference gene expression level [39].

Data analysis

Statistical analysis was conducted using Microsoft Excel 2010 (Microsoft, Redmond, WA, USA). The IBM SPSS Statistics software (version 26) was utilized for significance analysis of the data differences. An independent sample t-test was employed to compare the significance between the two data sets. For multiple data groups, the Waller-Duncan test in one-way ANOVA was used for multiple comparisons and significance difference analysis.

Results

Al stress inhibited the growth of peanut

From Fig. 1, we can see that as the concentration of aluminum increases, the growth of peanuts is increasingly restricted. Compared to the control group (0 mM Al), increasing Al treatment concentrations (0.4, 1.2, 4, and 10 mM Al) resulted in a reduction of the above-ground fresh weight of peanuts by 25.41%, 33.30%, 51.72%, and 61.15%, respectively. The fresh weight of roots decreased by 41.17%, 52.04%, 63.33%, and 63.84%. Total root length decreased by 62.27%, 79.32%, 85.70%, and 83.52%. Root surface area was reduced by 50.09%, 64.21%, 75.87%, and 75.37%. Conversely, the mean root diameter increased by 25.78%, 45.82%, 37.47%, and 28.31%. Total root volume decreased by 44.05%, 46.75%, 63.38%, and 68.88% (Table S3).

To investigate the effect of Al toxicity on peanut root tip growth, root tips treated with 0 mM (control group) and 4 mM Al (Al toxicity concentration) were observed using scanning electron microscopy (SEM). The apex of the root tip in the normal growth condition appeared triangular with numerous pores (Fig. 2A and B). In contrast, the root tip apex subjected to Al toxicity showed a smooth surface with a damaged vertex (Fig. 2C and D).

Changes of 4 physiological indexes in peanut leaves and roots under al stress

With 0 mM Al treatment as the control, the application of 0.4, 1.2, 4, and 10 mM Al for 20 days led to a significant increase in H_2O_2 content in leaves by 64.25%, 76.22%, 55.07%, and 55.23%, respectively (Fig. 3A). In roots, the H_2O_2 content increased significantly by 75.45% and 492.36% in the 4 and 10 mM treatment groups, respectively (Fig. 3B). PAL activity in leaves also increased significantly, showing increments of 20.37%, 30.32%, 68.26%, and 120.45% (Fig. 3C). In roots, PAL activity recorded increases of 14.95%, 45.12%, and 20.08% in the 1.2, 4, and 10 mM treatment groups, respectively (Fig. 3D). The T-AOC in leaves significantly increased by 42.89%, 72.30%, 211.35%, and 267.05% (Fig. 3E). However, T-AOC

Fig. 1 Growth effect of peanuts under different Al treatment concentrations. The peanuts were treated with different concentrations of Al for 20 days. (**A**) 0; (**B**) 0.4; (**C**) 1.2; (**D**) 4 and (**E**) 10 mM Al (Bar = 5 cm)

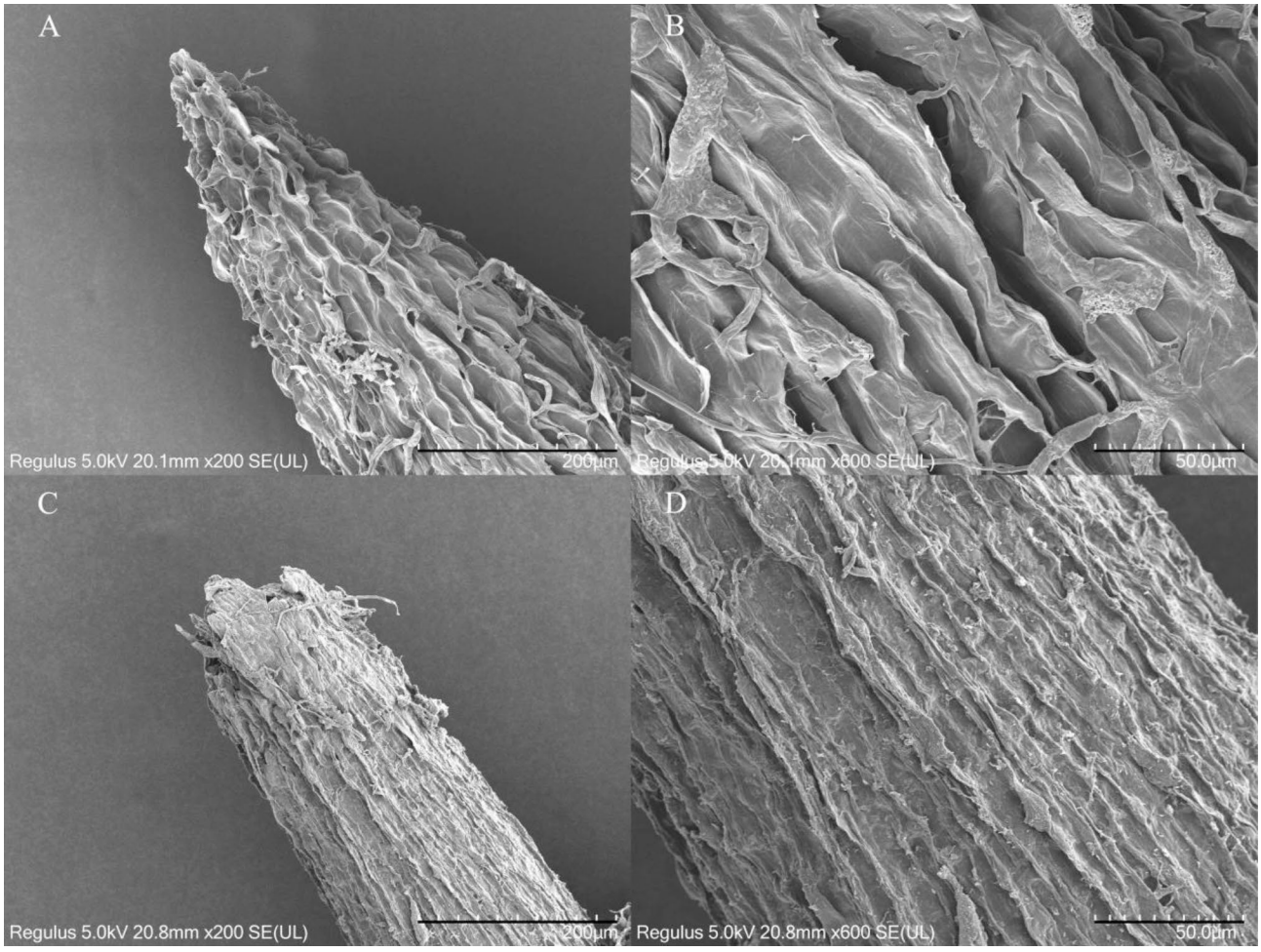

Fig. 2 SEM photos of root tips after 20 d treatment with 0 and 4 mM Al. (**A**) Root tip (Bar = 200 μm) and (**B**) epidermis (Bar = 50 μm) morphology after 0 mM Al treatment. (**C**) Root tip (Bar = 200 μm) and epidermis (Bar = 50 μm) morphology after 4 mM Al treatment

in roots decreased by 18.50% in the 1.2 mM group, with no significant changes in other treatment concentrations (Fig. 3F). In leaves, GSH content decreased significantly by 18.54%, 38.52%, and 16.75% in the 0.4, 1.2, and 4 mM treatment groups, respectively. Conversely, GSH content in the 10 mM treatment group increased significantly by 21.20% (Fig. 3G). In roots, GSH content increased significantly by 159.64%, 335.60%, and 398.52%, respectively in 1.2, 4, and 10 mM treatment (Fig. 3H).

Changes in the contents of 4 elements in peanut leaves and roots under Al stress

The contents of four elements in peanut leaves and roots were analyzed after 20 days of 0 and 4 mM Al treatment. Al content in leaves and roots increased significantly by 1008.44% (Fig. 4A) and 17477.26% (Fig. 4E), respectively. N content in leaves and roots decreased significantly by 23.67% (Fig. 4B) and 20.51% (Fig. 4F), respectively. P content did not change significantly in leaves (Fig. 4C) but increased significantly by 29.74% in roots (Fig. 4G). B content in leaves and roots decreased significantly by 39.47% (Fig. 4D) and 25.17% (Fig. 4H), respectively.

Changes of 4 hormone contents in peanut leaves and roots under al stress

The contents of four hormones in peanut leaves and roots were measured after 20 days of treatment with 0 and 4 mM Al. The content of IAA-ASP in leaves decreased significantly by 23.94% (Fig. 5A), whereas it increased significantly by 12.91% in roots (Fig. 5E). The content of Methyl jasmonate (MEJA) in leaves increased significantly by 2642.86% (Fig. 5B), but there was no significant change in roots (Fig. 5F). Methyl salicylate (MESA) content in leaves and roots increased significantly by 140.00% (Fig. 5C) and 472.22% (Fig. 5G), respectively. IPA content in leaves decreased significantly by 78.95% (Fig. 5D), and in roots, it decreased significantly by 20.66% (Fig. 5H).

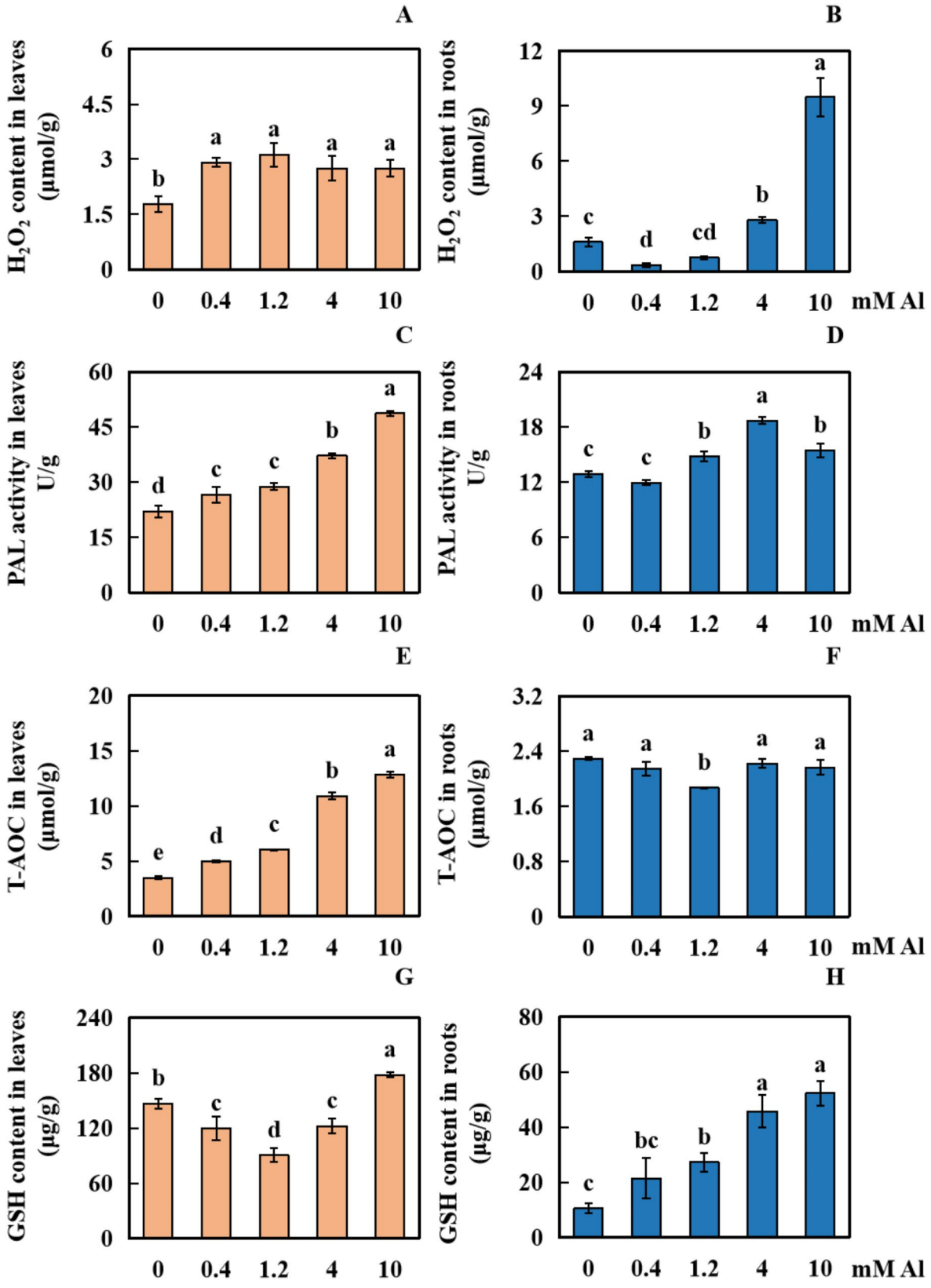

Fig. 3 (See legend on next page.)

(See figure on previous page.)

Fig. 3 Results of physiological response indexes of peanut leaves and roots under Al toxicity stress. The 4 physiological indexes of fresh peanut leaf and root samples from 0, 0.4, 1.2, 4, and 10 mM Al treated for 20 d. were determined. Hydrogen peroxide (H_2O_2) content of (**A**) leaves and (**B**) roots; Phenylalanine ammonia-lyase (PAL) activity of (**C**) leaves and (**D**) roots; Total antioxidant capacity (T-AOC) of (**E**) leaves and (**F**) roots; Reduced glutathione (GSH) content of (**G**) leaves and (**H**) roots. The results were expressed using the mean and standard deviation of three repeated biological experiments. Waller-Duncan multiple comparison test and one-way analysis of variance were used to compare the difference among all groups. Different letters on the bar chart indicated significant differences between data ($p < 0.05$)

Transcriptome analysis

Transcriptome sequencing and DEGs identification

After filtering low-quality data, we obtained an average of 48,371,552 clean reads from peanut leaf and root samples in both the control group (0 mM Al) and the Al treatment group (4 mM Al). Among all tested samples, the number of Clean Reads ranged from 40,094,710 to 64,575,446. The average percentage of clean reads was 98.81% (Table S4).

Figure S1A illustrates that the three biological replicates in each group clustered closely together, showing clear boundaries and good data reproducibility. Differential gene expression analysis revealed 5,831 DEGs in leaves and 6,405 DEGs in roots from peanuts treated with 4 mM Al. Differentially expressed genes (DEGs) were defined with the following criteria: $|\log_2\text{FoldChange}| > 1$ and a statistically significant P-value < 0.05. In total, 3,463 DEGs were up-regulated and 2,368 down-regulated in leaves, whereas 3,954 were up-regulated and 2,451 down-regulated in roots (Figure S1B). Additionally, 872 DEGs were up-regulated and 351 DEGs down-regulated in both leaves and roots. There were also 134 DEGs that were up-regulated in leaves but down-regulated in roots, and 124 DEGs that were down-regulated in leaves but up-regulated in roots (Figure S1C).

KEGG analysis of DEGs in peanut leaves and roots

Enrichment analysis was performed using the KEGG database, and 30 pathways (p-value < 0.05) with the most significant enrichment were selected for display to investigate the effects of Al toxicity stress on the DEGs in peanut leaves and roots. The enrichment pathways in peanut leaves were classified into four categories: cellular processes, environmental information processing, metabolism, and organismal systems (Fig. 6A). The primary enrichment pathways in leaves included phagosome, plant hormone signal transduction, plant circadian rhythm, starch and sucrose metabolism, nitrogen metabolism, glutathione metabolism, glyoxylate and dicarboxylate metabolism, vitamin B6 metabolism, and linoleic acid metabolism, among others (Fig. 6A). The enrichment pathways in peanut roots were classified into three categories: environmental information processing, metabolism, and organismal systems (Fig. 6B). The main enrichment pathways in roots included plant hormone signal transduction, plant circadian rhythm, phenylpropanoid synthesis, glutathione metabolism, cysteine and methionine metabolism, flavonoid biosynthesis, amino sugar and nucleotide sugar metabolism, isoflavonoid biosynthesis, tryptophan metabolism, and linoleic acid metabolism, among others (Fig. 6B).

Metabolome analysis

DAMs in peanut leaves and roots

The PCA of the peanut metabolomics profile is presented in Figure S2. The four independent biological replicates from the four sample groups clustered tightly together with distinct boundaries (Figure S2A).

A total of 314 DAMs were identified from leaf and root samples of the control group (0 mM Al) and the Al toxicity treatment group (4 mM Al). Of these, 210 DAMs were found in the leaves (103 up-regulated and 107 down-regulated), whereas 240 DAMs were detected in the roots (119 up-regulated and 121 down-regulated) (Figure S2B). In total, 32 DAMs were up-regulated in both leaves and roots, and 36 DAMs were down-regulated in both. Additionally, 37 DAMs were up-regulated in the leaves and down-regulated in the roots, whereas 31 were down-regulated in the leaves and up-regulated in the roots (Figure S2C).

To study the species differences of DAMs, we classified them separately for leaves and roots. In the leaves, the top five categories of DAMs were: Amino acids, peptides, and analogues (24), Fatty acids and conjugates (12), Carbohydrates and carbohydrate conjugates (10), Carbonyl compounds (10), and Alcohols and polyols (8) (Table S5). In the roots, the top five categories of DAMs were: Amino acids, peptides, and analogues (26), Carbohydrates and carbohydrate conjugates (18), Fatty acids and conjugates (14), Alcohols and polyols (13), and Carbonyl compounds (8) (Table S5).

KEGG functional enrichment analysis of differential metabolites

The KEGG enrichment pathway analysis and topological analysis identified the top 20 pathways with the highest enrichment in peanut leaves and roots (Fig. 7A and B). In leaves, DAMs were significantly enriched in "ABC transporters," "Linoleic acid metabolism," "Alanine, aspartate and glutamate metabolism," "Aminoacyl-tRNA biosynthesis," "D-Amino acid metabolism," etc. (Fig. 7A). In roots, DAMs were mass enriched in "Linoleic acid metabolism," "ABC transporters," "Phenylalanine metabolism,"

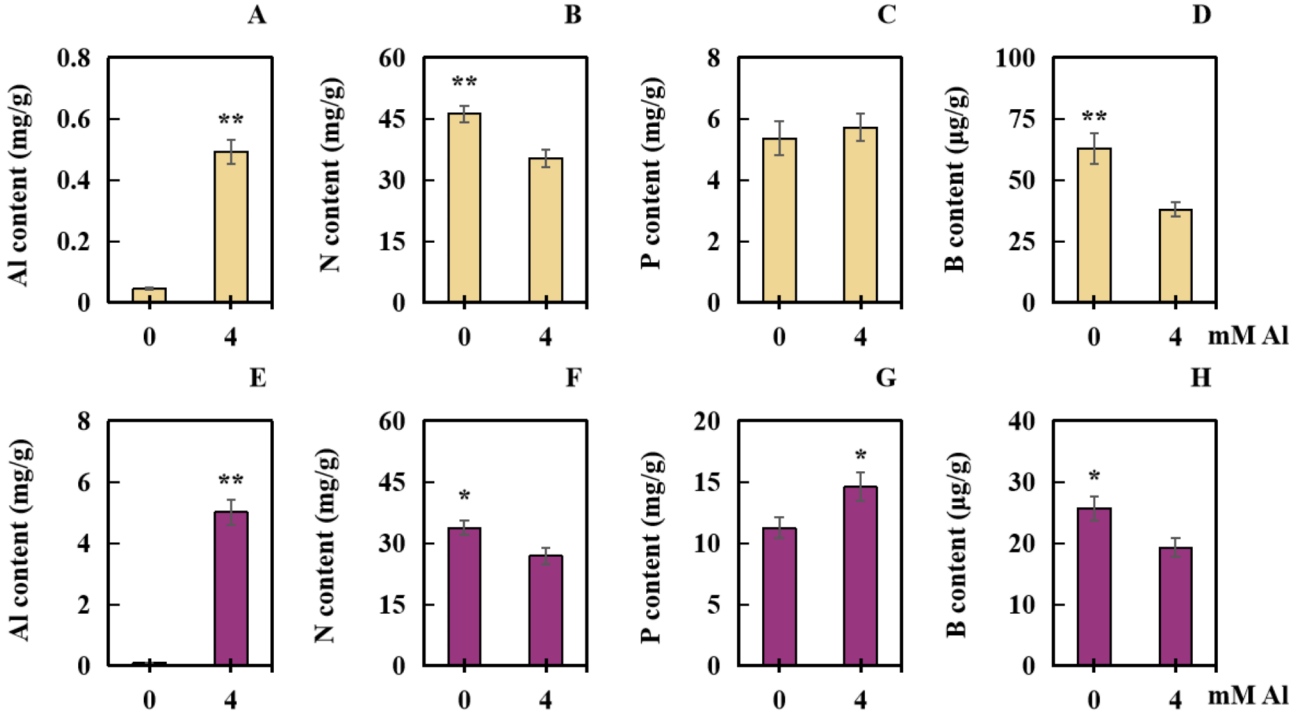

Fig. 4 Accumulation of 4 elements in peanut leaves and roots under Al toxicity stress. The contents of (**A**) Al, (**B**) N, (**C**) P, and (**D**) B in leaves. The contents of (**E**) Al, (**F**) N, (**G**) P, and (**H**) B in the roots. The data were expressed as the mean and standard deviation (SD) of three independent biological replicates. The significant difference between the control group and Al toxicity stress group was determined by independent sample T test (* $p < 0.05$, ** $p < 0.01$)

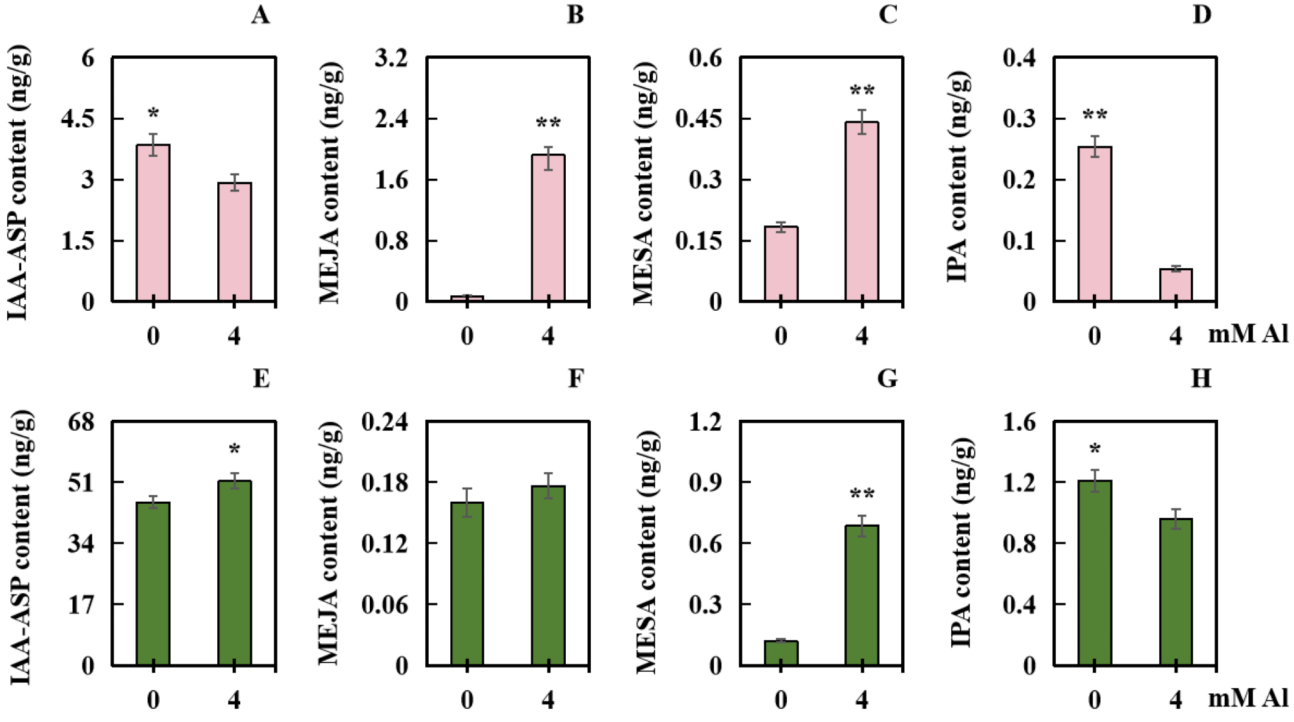

Fig. 5 Contents of 4 hormones in peanut leaves and roots under Al toxicity stress. The contents of (**A**) IAA-ASP, (**B**) MEJA, (**C**) MESA, and (**D**) IPA in leaves. The contents of (**E**) IAA-ASP, (**F**) MEJA, (**G**) MESA, and (H) IPA in roots. The data were expressed as the mean and standard deviation (SD) of three independent biological replicates. The significant difference between the control group and Al toxicity stress group was determined by independent sample T test (* $p < 0.05$, ** $p < 0.01$)

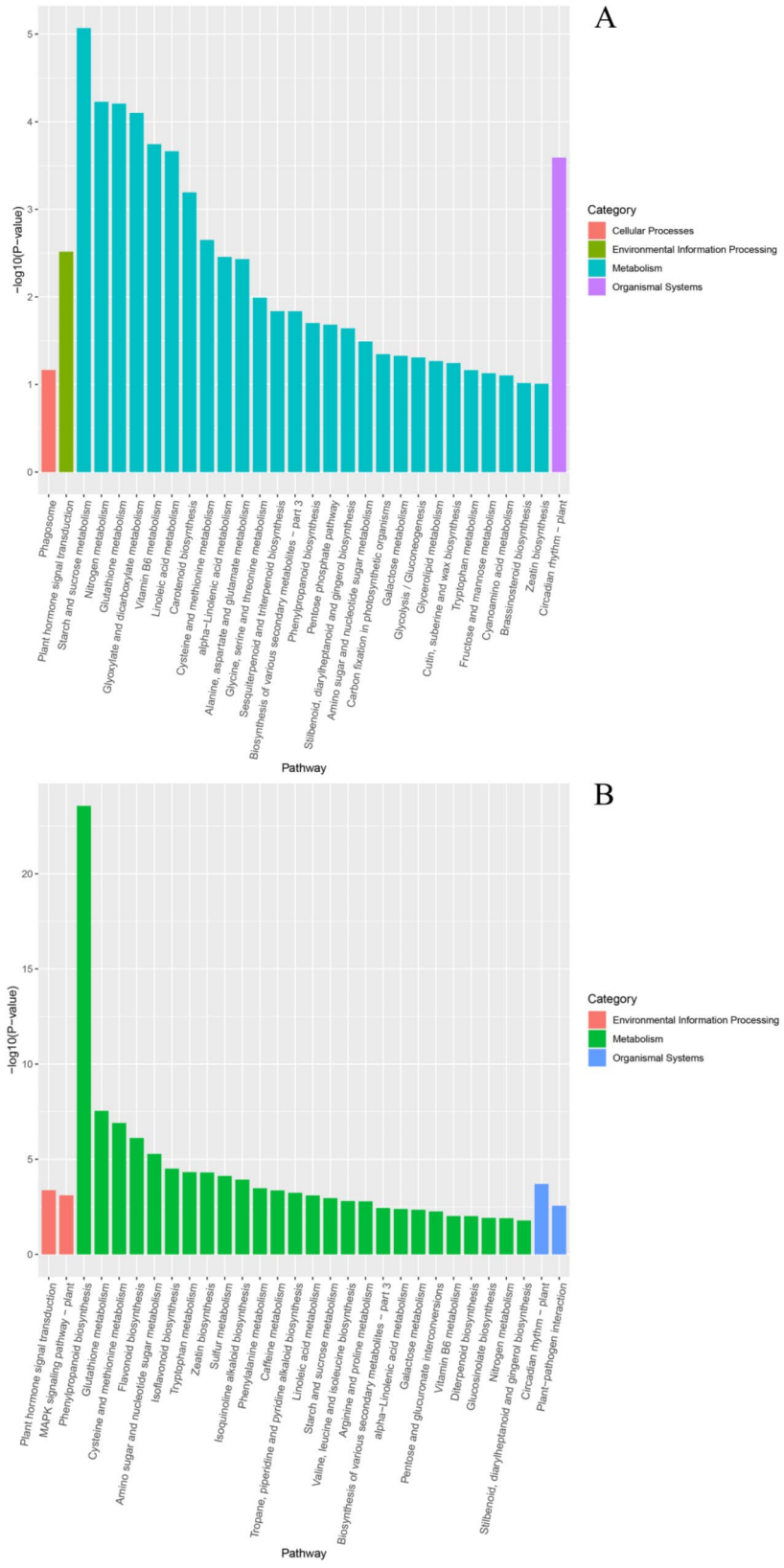

Fig. 6 KEGG enrichment analysis of DEGs. KEGG enrichment analysis of DEGs in peanut (**A**) leaves and (**B**) KEGG roots. The first 30 pathways with the lowest p-value, that was, the most significant enrichment, were selected for display. The horizontal coordinate was the pathway name, and the vertical coordinate was the enriched -log10 (p-value) of each pathway

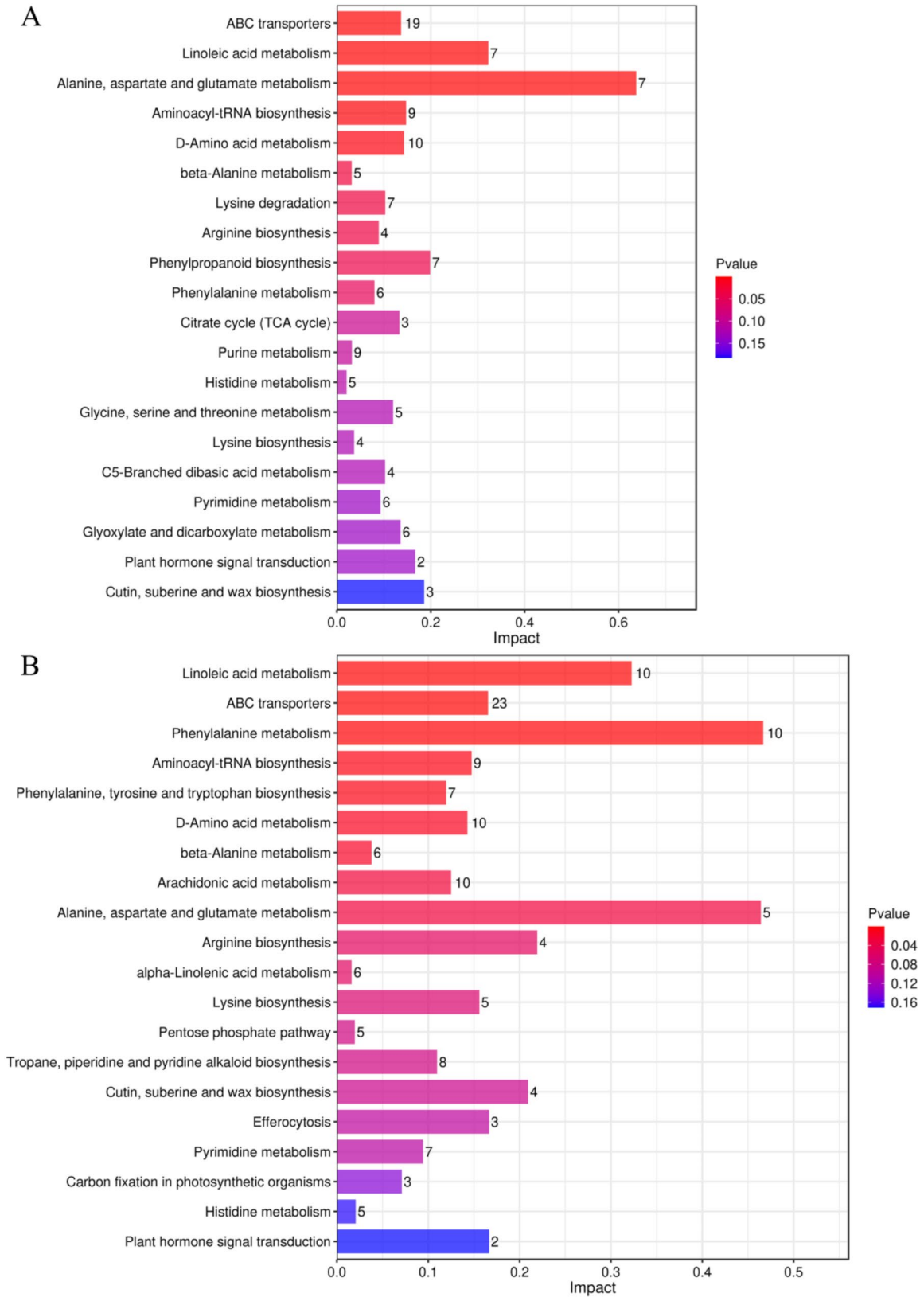

Fig. 7 (See legend on next page.)

(See figure on previous page.)

Fig. 7 KEGG enrichment analysis of DAMs. KEGG enrichment analysis of DAMs in peanut (**A**) leaves and (**B**) roots. The horizontal coordinate represented the impact value enriched into different pathways, and the higher the impact value, the higher the differential metabolite contribution detected in the pathway. The ordinates represented metabolic pathways. The number represented the corresponding amount of metabolite on the pathway. The redder of the bar chart represented the smaller of the P value, while the bluer of bar chart represented the larger of the P value. The smaller of the P-value meant the more significant the influence of detected DAMs on this pathway

"Aminoacyl-tRNA biosynthesis," "Phenylalanine, tyrosine and tryptophan biosynthesis," etc. (Fig. 7B).

Association analysis of transcriptome and metabolome

A joint analysis of the transcriptome and metabolome revealed three enrichment pathways in peanut leaves under Al toxicity stress (Fig. 8A and C), namely, "Alanine, aspartate and glutamate metabolism," "Linoleic acid metabolism," and "Phenylpropanoid biosynthesis" (Fig. 8C). 4 pathways were found enrichment in peanut roots (Fig. 8B and D), namely, "ABC transporters," "beta-Alanine metabolism," "Linoleic acid metabolism," and "Phenylalanine metabolism" (Fig. 8D).

Critical response path analysis

According to the results of a combined transcriptome and metabolome analysis, DEGs and DAMs were enriched in the "Linoleic Acid Metabolism" pathway in peanut roots and leaves (Fig. 9). In this pathway, enzymes associated with DEGs included TGL4 (2 DEGs down-regulated in leaves), CYP1A2 (2 DEGs down-regulated in roots), and LOX1-5 (6 DEGs up-regulated and 1 DEG down-regulated in leaves; 1 DEG up-regulated and 7 DEGs down-regulated in roots). Additionally, LOX2S showed 2 DEGs up-regulated and 2 DEGs down-regulated in leaves, as well as 4 DEGs down-regulated in roots. Analysis of DAMs in this pathway revealed that γ-linolenate, linoleate, and 13(S)-HODE were down-regulated only in leaves. Conversely, dihomγ-linolenate and 9(S)-HODE were up-regulated only in roots. The compounds 12,13-DHOME, 9,10-DHOME, 9-OxoODE, and 13-OxoODE were down-regulated exclusively in roots. Both 9,10–12,13-diepoxy-octadecanoate and 9(S)-HPODE were up-regulated in both leaves and roots. Arachidonate and 13(S)-HPODE were up-regulated in leaves whereas being down-regulated in roots. Detailed information of DEGs and DAMs in the Linoleic Acid Metabolism pathway is provided in Table S6 and Table S7.

Additionally, we randomly selected some DEGs in the linoleic acid metabolism pathway of leaves and roots for validation using qRT-PCR, with the results and primer information detailed in Figure S3 and Table S8. The results showed that the up- and down-regulation changes of DEGs validated by qRT-PCR were consistent with the transcriptome data, indicating that the transcriptome results have good reliability.

Discussion

Phenotype and physiology

Peanut root growth was significantly inhibited after exposure to Al toxicity. This inhibition may be attributed to excess Al binding tightly to the cell walls of plant root cells, resulting in decreased cell wall ductility and ultimately impacting root development [6]. A similar phenomenon was observed in eucalyptus clone roots under Al stress [4].

Abiotic stress often results in excessive accumulation of ROS in cells [40]. In peanut leaves and roots, high levels of ROS, particularly H_2O_2, cause significant oxidative damage. As Al concentration rises, the antioxidant system struggles to eliminate the excess ROS, leading to sustained high H_2O_2 levels in peanuts. A similar trend in H_2O_2 content is observed in the leaves of Vitis vinifera under cadmium (Cd) stress [41]. T-AOC includes various antioxidant substances and enzymes, is crucial for plants facing heavy metal stress. The T-AOC level in plants correlates with the extent of oxidative damage they experience [42]. Despite increasing Al levels, peanuts can adapt to Al toxicity by enhancing T-AOC in their leaves. *Poncirus trifoliata* has also been shown to resist Al stress by increasing T-AOC [43]. However, the accumulation of Al in roots can lead to a surge in ROS, risking severe damage to the antioxidant defense system and complicating changes in T-AOC. Changes in PAL activity serve as biochemical indicators of plant responses to environmental stress [44]. PAL possesses antioxidant traits that enable it to neutralize ROS through the synthesis of phenolic compounds [44]. Increased PAL activity has also been noted in the roots of Cd-treated rice (*Oryza sativa*) [45]. Furthermore, PAL plays a key role in enhancing plant resistance by influencing lignin synthesis and increasing lignification in plant tissues [46]. In this study, the increase in average root diameter of peanuts may be associated with the rise in PAL activity. Reduced GSH is an essential non-enzymatic compound that directly or indirectly removes ROS. This small antioxidant molecule, formed during sulfur metabolism, binds to metal ions, producing phytochelatin peptides that enhance plant tolerance to specific metals [47, 48]. Research indicates that higher GSH levels in tolerant rice roots aid in coping with Al toxicity stress [48].

Electron microscopy observations reveal the root tip of peanuts has a loose and porous surface. After exposure to Al toxicity, the root cap of the peanut root tip becomes damaged, resulting in a denser and smoother surface.

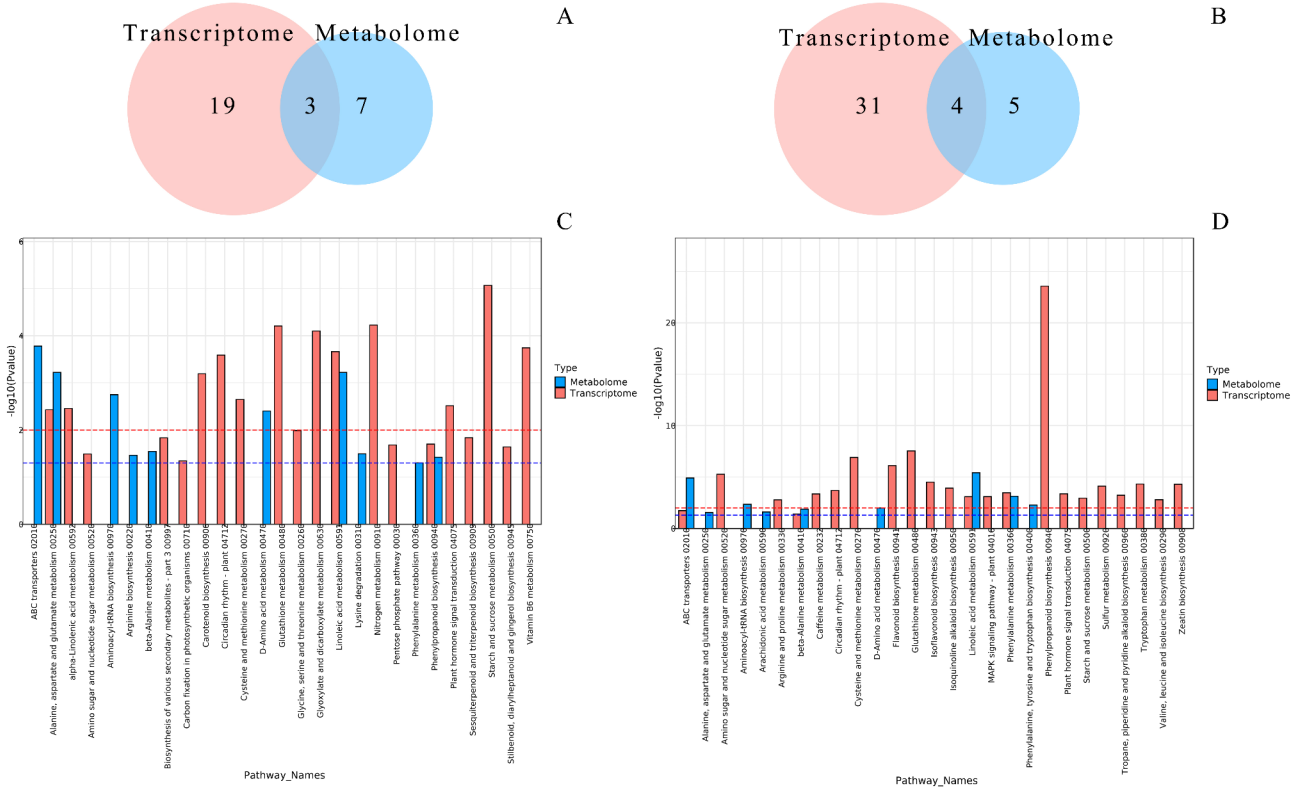

Fig. 8 Screening of key regulatory pathways in peanut leaves and roots in response to Al toxicity stress. Wayne diagram of KEGG enrichment association after transcriptome and metabolome conjoint analysis in (**A**) leaves and (**B**) roots. Different color regions represented the number of KEGG enrichment pathways in different omics, and overlapping regions represent the number of pathways enriched in the two omics. KEGG enrichment histogram of transcriptome and metabolome conjoint analysis in (**C**) leaves and (**D**) roots. According to the enrichment analysis results of DAMs and differential mRNA, histogram was used to show the significance of the enrichment pathway. It was sorted according to the P. value from smallest to largest. The first 20 results of DAMs and differential mRNA pathway enrichment were selected respectively

This alteration may hinder nutrient absorption. Similarly, in *Trifolium repens*, Al toxicity-induced morphological changes at the root tip lead to reduced nutrient content in the roots [49].

Accumulation of Al and absorption of N, P and B

After Al treatment, peanuts showed increased Al accumulation in both leaves and roots, with root Al levels being significantly higher than those in leaves. This may be attributed to the root system's initial exposure to Al ions, which can more readily bind to de-esterified pectin in the cell wall, ultimately becoming fixed there [5]. Excessive Al in the cytoplasm can lead to various chromosomal abnormalities, such as chromosome adhesion, hysteresis, micronuclei, binucleate, and multinucleate cells, adversely affecting plant cell division and differentiation [50]. Nitrogen is a vital macronutrient essential for plants' normal growth and development, influencing crop yield and quality [51]. The N content in peanut leaves and roots was significantly reduced under Al toxicity stress. This decline may result from changes in the expression of nitrogen metabolism-related enzymes (such as nitrate reductase [NR], glutathione synthetase [GS], and glutamine-2-oxoglutarate aminotransferase [GOGAT]) and associated genes (includes NR, GS1, FD-GOGAT, and glutamate dehydrogenase [GDH]), which ultimately disrupt nitrogen metabolism [52]. It has been suggested that plants with a greater preference for ammonium nitrogen may exhibit higher resistance to Al toxicity stress compared to those reliant on nitrate nitrogen [53]. P is another crucial macronutrient, playing a significant role in synthesizing macromolecules like nucleic acids, phospholipids, ATP, and NADP [54]. Under Al toxicity, the P content in roots increased significantly. Similar patterns have been observed in *Camellia japonica*, where root P content rose after Al stress [55]. This increase may be due to Al toxicity affecting acid phosphatase activity and polyphosphate utilization, thereby altering phosphorus absorption efficiency [56]. Additionally, enhanced P absorption can mitigate protein synthesis inhibition and promote carbohydrate accumulation, aiding plants in alleviating Al toxicity damage [54]. Boron (B) is an essential nutrient for higher plants [57]. B aids in the cross-linking of rhamnose-galacturonoglycan in plant cell walls via diester bonds, contributing to the formation of stable cell walls [58, 59]. A well-structured network of cell

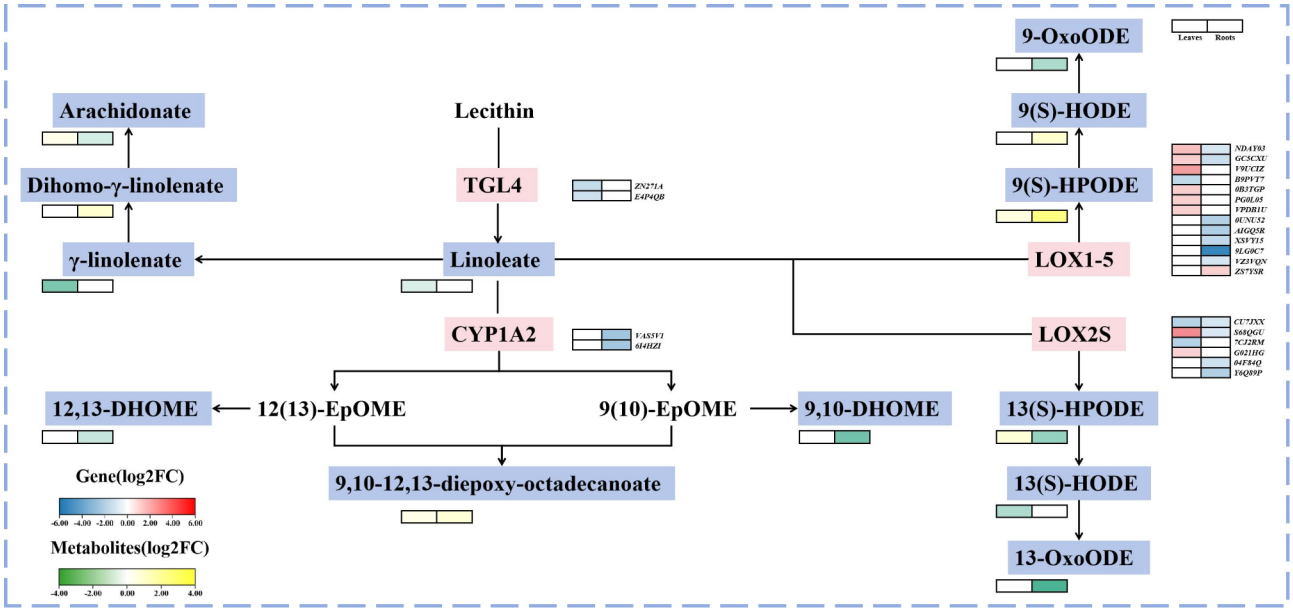

Fig. 9 Analysis of regulatory pathways of linoleic acid metabolism in peanut leaves and roots under Al toxicity stress. The blue color blocks represented the DAMs, and the pink color blocks represented the related enzymes affected by the DEGs. Smaller adjacent rectangles represented heat maps of DEGs or DAMs. The rectangles were divided into two equal parts (leaves on the left, roots on the right), the color of the rectangles indicated that the genes or metabolites were regulated under Al toxicity treatment, as shown on the scale, and the white rectangles indicated metabolites or genes that were not differentially expressed. TGL4: TAG lipase / steryl ester hydrolase / phospholipase A2 / LPA acyltransferase; CYP1A2: Cytochrome P450 family 1 subfamily A2; LOX1-5: Linoleate 9 S-lipoxygenase; LOX2S: Lipoxygenase. 12,13-DHOME: (9Z)-12,13-Dihydroxyoctadec-9-enoic acid; 9,10-DHOME: (12Z)-9,10-Dihydroxyoctadec-12-enoic acid; 9-OxoODE: (10E,12Z)-9-Oxooctadeca-10,12-dienoic acid; 9(S)-HODE: (10E,12Z)-(9 S)-9-Hydroxyoctadeca-10,12-dienoic acid; 9(S)-HPOD: (10E,12Z)-(9 S)-9-Hydroperoxyoctadeca-10,12-dienoic acid; 13(S)-HPODE: (9Z,11E)-(13 S)-13-Hydroperoxyoctadeca-9,11-dienoic acid; 13(S)-HODE: (9Z,11E)-(13 S)-13-Hydroxyoctadeca-9,11-dienoic acid; 13-OxoODE: (9Z,11E)-13-Oxooctadeca-9,11-dienoic acid

wall components can limit the entry of toxic substances, including Al. In *Poncirus trifoliata*, B was found to regulate pectin methylation levels and hemicellulose content in the cell wall, thereby mitigating Al toxicity damage [43]. A deficiency in B may weaken the defensive capacity of peanut cell walls.

Regulation of several hormones under Al

The IAA amino acid conjugate IAA-ASP is a storage form of IAA [60]. IAA regulates all aspects of normal plant growth and development through its synthesis, metabolism, polar transport, and signal transduction [61]. The stability of IAA levels reflects how plants respond to environmental changes [62, 63]. Metal ions influence the metabolism and dynamic polar distribution of IAA [61]. The acylamide synthase encoded by the GH3 gene converts IAA to IAA-ASP. This conversion can be reversed by amide hydrolase, which is regulated by the ILR1/ILL gene [60]. Excessive Al ions may disrupt the expression of related genes, affecting the equilibrium between IAA and IAA-ASP. Both MeJA and jasmonic acid (JA) are part of the JA family. They play significant roles in plant growth processes, such as proliferation, differentiation, secondary metabolite accumulation, and environmental stress tolerance [64, 65]. Increased MeJA content helps plants cope with metal ion stress. For instance, under Cd stress, applying exogenous MeJA enhanced the hormone metabolic function in *Abelmoschus esculentus*, increased the levels of osmoregulatory substances, improved photosynthetic pigment function, and boosted the plant's ability to clear H_2O_2 [66]. MeSA, a derivative of salicylic acid (SA), is produced when methyltransferase reacts with SA. Both MeSA and SA are signaling molecules in plant immune and defense networks [67]. Appropriate concentrations of MeSA applied to salt-stressed rice can enhance its total flavonoid content [68]. An increase in MeSA in peanut leaves and roots can help them adapt to Al toxicity stress. Numerous types of cytokinins exist in plants, with IPA being one of the most common. IPA can induce cell division and proliferation, playing a vital role in bud or bulb formation [69, 70]. An increase in IPA content has helped *Zanthoxylum bungeanum* cope with low temperature stress and allowed *Citrus sinensis* to adapt to Al toxicity stress [71, 72]. Conversely, IPA content decreased in peanut leaves and roots, likely due to high Al concentration. A similar decrease in IPA content was observed in *Arabidopsis thaliana* under severe arsenic trivalent stress [73].

Key pathways for transcriptome and metabolome screening

Integration of biomics data revealed three KEGG pathways in leaves that are common to both transcriptomic and metabolomic levels: alanine, aspartate, and glutamate metabolism; linoleic acid metabolism; and phenylpropanoid biosynthesis. In the root system, four KEGG pathways were identified as shared between transcriptomic and metabolomic levels: "ABC transporters", "beta-alanine metabolism", linoleic acid metabolism", and phenylalanine metabolism. Notably, "linoleic acid metabolism" is a pathway common to both leaves and roots and has been identified as a key pathway in peanut's response to Al toxicity stress.

Al exposure caused alterations in the metabolic pathway of linoleic acid in peanuts. Arachidonate, a signaling molecule, regulates the stress signaling network in plants. An increase in its content may trigger defense-related responses [74]. Linoleate converts to gamma-linolenate, which then transforms into dihomo-gamma-linolenate, ultimately resulting in arachidonate. Following Al exposure, the expression of TGL4-related genes was down-regulated, leading to a reduction in linoleate content. Consequently, the levels of gamma-linolenate and dihomo-gamma-linolenate were also affected. Arachidonate content increased in the leaves but decreased in the roots. Notably, the trend for arachidonate content differed from that of gamma-linolenate and dihomo-gamma-linolenate, potentially due to Al ions affecting other factors involved in arachidonate synthesis. Lipid oxidation products, known as oxylipids, serve as signaling molecules that aid plant defenses against stress. In higher plants, linolenate is a primary source of these compounds [75]. Derivatives such as 9,10-DHOME, 12,13-DHOME, and 9,10–12,13-diepoxy-octadecanoate can serve as markers of oxidation status and are crucial for plant development and defense [76]. The down-regulated expression of CYP1A2-related genes in peanut roots under Al toxicity may lead to decreased levels of 9,10-DHOME and 12,13-DHOME. However, the content of 9,10–12,13-diepoxy-octadecanoate increased in both leaves and roots, which may not correlate directly with the altered expression of CYP1A2-related genes. Linoleic acid can be converted into 9- and 13-hydroperoxide derivatives, depending on the specific lipoxygenases (LOXs) involved [77]. Differential expression of LOX1-5 and LOX2S-related genes following Al toxicity caused abnormal conversion of linolenate to 9(S)-HPODE and 13(S)-HPODE via lipoxygenase. As a result, the levels of secondary metabolites (9(S)-HODE, 9-Oxoode, 13(S)-HODE, and 13-Oxoode) were down-regulated. Similar changes have been observed in Cd-stressed *Lolium perenne* [78]. However, the up- and down-regulation patterns of LOX1-5 and LOX2S-related genes were inconsistent with the corresponding secondary metabolite levels. This suggests that Al may influence the linoleic acid metabolic pathway through both enzymatic and non-enzymatic mechanisms.

The unsaturated fatty acids, including linoleic acid, present in the cell membrane help regulate membrane fluidity and signal transduction to maintain cellular function [79]. Unsaturated fatty acids are highly sensitive to ROS and frequently undergo oxidative reactions with ROS, leading to membrane lipid peroxidation and oxidative damage in plant cells [80, 81]. Excessive aluminum mediates elevated ROS levels, and persistent membrane lipid peroxidation results in continuous lipid depletion and excessive generation of lipid hydroperoxides, ultimately disrupting the structural integrity of the plasma membrane and reducing its fluidity [82, 83]. During the ROS-induced damage to unsaturated fatty acids, the linoleic acid metabolic pathway is also severely affected, which may explain why DEGs and DAMs are enriched in the linoleic acid metabolism pathway.

Potential mechanism of peanut response to Al toxicity stress

According to the experimental results of this study, Fig. 10 illustrates the potential regulatory mechanisms of peanut leaf and root responses to Al toxicity. First, high levels of exogenous Al increased the Al content in both leaves and roots (Fig. 10I). Excessive Al accumulation led to elevated intracellular ROS, as indicated by H_2O_2 levels (Fig. 10III and IV), resulting in significant oxidative damage (Fig. 10I). This cellular damage further impaired the root system's ability to absorb nutrients (Fig. 10II). In response to high Al concentrations, peanuts activated their cellular defense mechanisms, which included three main aspects: physiological responses (Fig. 10V), hormonal regulation (Fig. 10VII), and molecular regulation (Fig. 10VI). Peanuts adapted to the high Al stress by regulating DEGs, particularly those related to lipoxygenase in the linoleic acid metabolic pathway (Fig. 10VIII), and by accumulating metabolites such as linoleic acid peroxides (Fig. 10IX). Despite these adaptive changes, peanut growth remained constrained due to Al toxicity.

Conclusion

Al treatment significantly inhibited peanut growth. It resulted in considerable accumulation of Al in both leaves and roots, increased H_2O_2 content, ROS accumulation, and a responsiveness of the antioxidant system. Additionally, the content of plant hormones such as IAA-Asp, MeJA, MeSA, and IPA was affected in leaves and roots. Al toxic stress also hindered the uptake of essential nutrients, including N, P, and B. Comprehensive transcriptomic and metabolomic analyses revealed that the "linoleic acid metabolism" pathway was notably

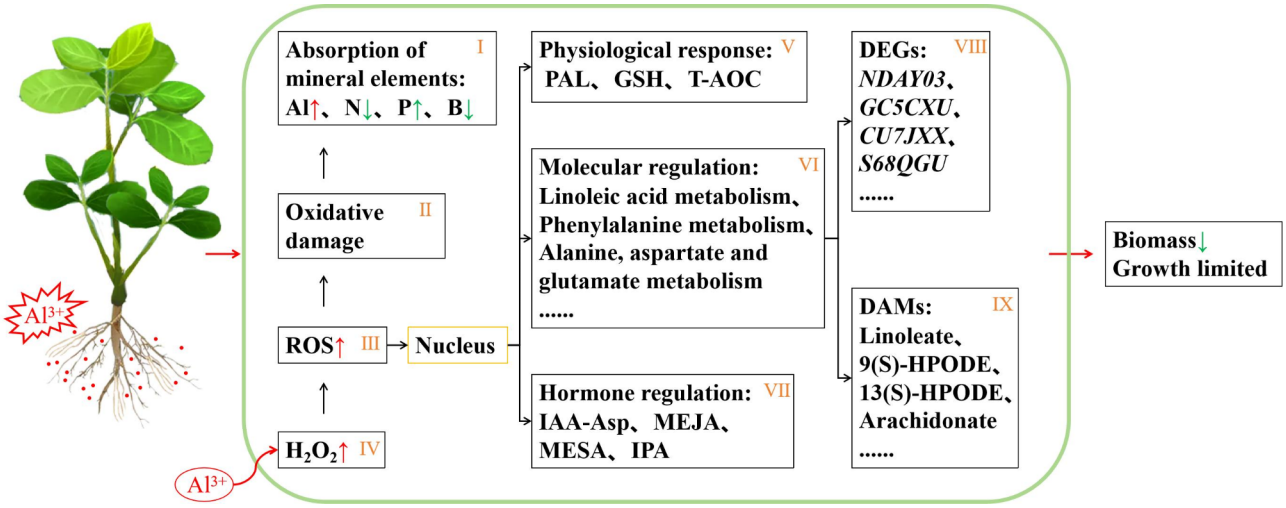

Fig. 10 Potential regulatory mechanisms in peanut leaves and roots under Al toxicity stress (I) The change of mineral element absorption; (II) The cells were damaged by oxidation; (III) Intracellular reactive oxygen species level; (IV) Change of hydrogen peroxide content; (V) Several physiological indicators related to stress resistance; (VI) Main pathways of molecular regulation; (VII) Changes in the content level of several hormones; (VIII) DEGs in the pathway; (IX) DAMs in the pathway. Small red arrows indicated an increase in substance content. Small green arrows indicated a reduction in substance content

enriched in peanut leaves and roots under Al toxicity stress. LOX plays a crucial role in the oxidation of linoleic acid, with genes LOX1-5 and LOX2S being differentially expressed in both leaves and roots. These genes regulate the oxidized derivatives of linoleic acid and help mitigate oxidative damage. In summary, this study elucidated the complex physiological and molecular mechanisms of peanuts under Al poisoning stress and highlighted the significance of linoleic acid metabolism in coping with Al toxicity. These findings enhance our understanding of the effects of Al toxicity on peanut development and the response of key metabolic pathways, providing potential molecular targets for genetic engineering to improve crop resistance to Al stress.

Abbreviations

DEGs	Differentially Expressed Genes
DAMs	Differentially Accumulated Metabolites
SEM	Scanning Electron Microscopy
T-AOC	Total Antioxidant Capacity
PAL	Phenylalanine Ammonia Lyase
GSH	Reduced Glutathione
IAA-Asp	Indole-3-Acetic Acid-Aspartate
MeJA	Methyl Jasmonate
MeSA	Methyl Salicylate
IPA	Isopentenyl Adenosine.

Supplementary Information

The online version contains supplementary material available at https://doi.org/10.1186/s12870-025-06460-7.

Supplementary Material 1: Figure S1: Al toxicity stress induces changes in the transcriptome of peanuts; Figure S2: Al toxicity stress induces changes in the metabolic profile of peanuts; Figure S3: qRT-PCR validation of DEGs in the linoleic acid pathway.

Supplementary Material 2: Table S1: Composition and content in hydroponic solution; Table S2: Plant hormone detection parameter setting; Table S3: Parameters of peanut growth; Table S4: Statistics for evaluation of sequencing data for peanut leaf and root samples; Table S5: The top 5 classes of DAMs in peanut leaves and roots; Table S6: DEGs in linoleic acid metabolism pathway; Table S7: DAMs in linoleic acid metabolism pathway; Table S8: qRT-PCR primers in linoleic acid metabolism pathway.

Acknowledgements
We would like to thank the Analytical and Testing Center of Guangdong Ocean University for the determination of ion contents.

Author contributions
J.S., Y.Z. and Y.L.: Conceived and designed the experiments. J.S., Y.Z., S.Y., Y.X., Y.W., H.H., and Y.L.: Performed the experiments and analyzed the data. J.S., Y.Z., and Y.L.: Wrote the manuscript. All authors have read and agreed to the published version of the manuscript.

Funding
This research was funded by the Project of Rural Science and Technology Team "One-to-One" Service to Help the Town Full Coverage of Action Funding in Zhanjiang City (A23081), the Project of Social Services of Rural Science and Technology Specialists of Guangdong Ocean University (080503052212), the Graduate Education Innovation Program of Guangdong Ocean University (202401), and the Project of Jiaying University/Guangdong Provincial Key Laboratory of Conservation and Precision Utilization of Characteristic Agricultural Resources in Mountainous Areas (2023JYKF05).

Data availability
The raw sequencing data of the transcriptomics in this study can be found in the NCBI database under registration number PRJNA1175555 (https://www.ncbi.nlm.nih.gov/bioproject/PRJNA1175555).

Declarations

Ethics approval and consent to participate
Not applicable.

Consent for publication
Not applicable.

Competing interests
The authors declare no competing interests.

Received: 1 January 2025 / Accepted: 25 March 2025

Published online: 07 April 2025

References

1. Qi S, Li X, Luo J, Han R, Chen Q, Shen D, Shentu J. Soil heterogeneity influence on the distribution of heavy metals in soil during acid rain infiltration: experimental and numerical modeling. J Environ Manage. 2022;322:116144.
2. Bojórquez-Quintal E, Escalante-Magaña C, Echevarría-Machado I, Martínez-Estévez M. Aluminum, a friend or foe of higher plants in acid soils. Front Plant Sci. 2017;8:1767.
3. Xu S, Wu L, Li L, Zhong M, Tang Y, Cao G, Lin K, Ye Y. Aluminum-induced alterations to the cell wall and antioxidant enzymes involved in the regulation of the aluminum tolerance of Chinese Fir (*Cunninghamia lanceolata*). Front. Plant Sci. 2022;13:891117.
4. Li W, Ullah S, Xu Y, Bai T, Ye S, Jiang W, Yang M. Effects of elevated aluminum concentration and distribution on root damage, cell wall polysaccharides, and nutrient uptake in different tolerant Eucalyptus clones. Int J Mol Sci. 2022;23(21):13438–13438.
5. Sun C, Lu L, Yu Y, Liu L, Hu Y, Ye Y, Jin C, Lin X. Decreasing methylation of pectin caused by nitric oxide leads to higher aluminium binding in cell walls and greater aluminium sensitivity of wheat roots. J Exp Bot. 2016;67(3):979–89.
6. Singh S, Tripathi DK, Singh S, Sharma S, Dubey NK, Chauhan DK, Vaculík M. Toxicity of aluminium on various levels of plant cells and organism: a review. Environ Exp Bot. 2017;137:177–93.
7. Donnelly CP, De Sousa A, Cuypers B, Laukens K, Al-Huqail AA, Asard H, Beemster GT, AbdElgawad H. Malate production, sugar metabolism, and redox homeostasis in the leaf growth zone of Rye (*Secale cereale*) increase stress tolerance to aluminum stress: A biochemical and genome-wide transcriptional study. J Hazard Mater. 2024;464:132956.
8. De Sousa A, AbdElgawad H, Fidalgo F, Teixeira J, Matos M, Tamagnini P, Fernandes R, Figueiredo F, Azenha M, Teles LO, Korany SM. Subcellular compartmentalization of aluminum reduced its hazardous impact on Rye photosynthesis. Environ Pollut. 2022;315:120313.
9. Peixoto HP, Da Matta FM, Da Matta JC. Responses of the photosynthetic apparatus to aluminum stress in two sorghum cultivars. J Plant Nutr. 2002;25(4):821–32.
10. Wang L, Fan XW, Pan JL, Huang ZB, Li YZ. Physiological characterization of maize tolerance to low dose of aluminum, highlighted by promoted leaf growth. Planta. 2015;242(6):1391–403.
11. Kochian LV, Piñeros MA, Liu J, Magalhaes JV. Plant adaptation to acid soils: the molecular basis for crop aluminum resistance. Annu Rev Plant Biol. 2015;66(1):571–98.
12. Ofoe R, Thomas RH, Asiedu SK, Wang-Pruski G, Fofana B, Abbey L. Aluminum in plant: benefits, toxicity and tolerance mechanisms. Front Plant Sci. 2023;13:1085998.
13. Kichigina NE, Puhalsky JV, Shaposhnikov AI, Azarova TS, Makarova NM, Loskutov SI, Safronova VI, Tikhonovich IA, Vishnyakova MA, Semenova EV, Kosareva IA. Aluminum exclusion from root zone and maintenance of nutrient uptake are principal mechanisms of al tolerance in *Pisum sativum* L. Physiol. Mol Biol Plants. 2017;23(4):851–63.
14. Geng X, Horst WJ, Golz JF, Lee JE, Ding Z, Yang ZB. LEUNIG _ HOMOLOG transcriptional co-repressor mediates aluminium sensitivity through PECTIN METHYLESTERASE 46-modulated root cell wall pectin methylesterification in Arabidopsis. Plant J. 2017;90(3):491–504.
15. Wu Q, Tao Y, Huang J, Liu YS, Yang XZ, Jing HK, Shen RF, Zhu XF. The MYB transcription factor MYB103 acts upstream of TRICHOME BIREFRINGENCE-LIKE27 in regulating aluminum sensitivity by modulating the O-acetylation level of cell wall Xyloglucan in *Arabidopsis Thaliana*. Plant J. 2022;111(2):529–45.
16. Takeuchi J, Fukui K, Seto Y, Takaoka Y, Okamoto M. Ligand–receptor interactions in plant hormone signaling. Plant J. 2021;105(2):290–306.
17. Jia Y, Yu P, Shao W, An G, Chen J, Yu C, Kuang H. Up-regulation of *LsKN1* promotes cytokinin and suppresses Gibberellin biosynthesis to generate wavy leaves in lettuce. J Exp Bot. 2022;73(19):6615–29.
18. Miao Y, Luo X, Gao X, Wang W, Li B, Hou L. Exogenous Salicylic acid alleviates salt stress by improving leaf photosynthesis and root system architecture in cucumber seedlings. Sci Hortic. 2020;272:109577.
19. Ulloa-Inostroza EM, Alberdi M, Meriño-Gergichevich C, Reyes-Díaz M. Low doses of exogenous Methyl jasmonate applied simultaneously with toxic aluminum improve the antioxidant performance of *Vaccinium corymbosum*. Plant Soil. 2017;412:81–96.
20. Wu BS, Zhang J, Huang WL, Yang LT, Huang ZR, Guo J, Wu J, Chen LS. Molecular mechanisms for pH-mediated amelioration of aluminum-toxicity revealed by conjoint analysis of transcriptome and metabolome in *Citrus sinensis* roots. Chemosphere. 2022;299:134335.
21. Wu BS, Huang WT, Rao RY, Chen WS, Hua D, Lai NW, Wu J, Yang LT, Chen LS. Integrated analysis of transcriptome, metabolome and physiology revealed the molecular mechanisms for elevated pH-mediated-mitigation of aluminum-toxicity in *Citrus sinensis* leaves. Sci Hortic. 2023;322:112391.
22. Wang J, Su C, Cui Z, Huang L, Gu S, Jiang S, Feng J, Xu H, Zhang W, Jiang L, Zhao M. Transcriptomics and metabolomics reveal tolerance new mechanism of rice roots to al stress. Front Genet. 2023;13:1063984.
23. Li C, Shi H, Xu L, Xing M, Wu X, Bai Y, Niu M, Gao J, Zhou Q, Cui C. Combining transcriptomics and metabolomics to identify key response genes for aluminum toxicity in the root system of *Brassica Napus* L. seedlings. Theor Appl Genet. 2023;136(8):169.
24. Liao BS. Current situation and potential analysis of peanut production in China. Chin J Oil Crop Sci. 2020;42:161–6. (In Chinese).
25. Yan ML, Ge WW, Zhang X, Huang YN, Zhang ZD, Zhang Y. The situation analysis and development of oil industry in China countermeasures. China Oils Fats. 2023;48:8–18. (In Chinese).
26. Xiao D, Li X, Zhou YY, Wei L, Keovongkod C, He H, Zhan J, Wang AQ, He LF. Transcriptome analysis reveals significant difference in gene expression and pathways between two peanut cultivars under al stress. Gene. 2021;781:145535.
27. Liu Y, Xue Y, Xie B, Zhu S, Lu X, Liang C, Tian J. Complex gene regulation between young and old soybean leaves in responses to manganese toxicity. Plant Physiol Biochem. 2020;155:231–42.
28. Yan J, Zhu W, Wu D, Chen X, Yang S, Xue Y, Liu Y. Mechanisms of aluminum toxicity impacting root growth in *Shatian pomelo*. Int J Mol Sci. 2024;25(24):13454.
29. Wang Y, Li J, Pan Y, Chen J, Liu Y. Metabolic responses to manganese toxicity in soybean roots and leaves. Plants. 2023;12(20):3615.
30. Kalogiouri NP, Manousi N, Zachariadis GA. Determination of the toxic and nutrient element content of almonds, walnuts, hazelnuts and pistachios by ICP-AES. Separations. 2021;8(3):28.
31. Chen Z, Cui Q, Liang C, Sun L, Tian J, Liao H. Identification of differentially expressed proteins in soybean nodules under phosphorus deficiency through proteomic analysis. Proteomics. 2011;11(24):4648–59.
32. Khew CY, Mori IC, Matsuura T, Hirayama T, Harikrishna JA, Lau ET, Augustine Mercer ZJ, Hwang SS. Hormonal and transcriptional analyses of fruit development and ripening in different varieties of black pepper (*Piper nigrum*). J Plant Res. 2020;133:73–94.
33. Liu Y, Pan Y, Li J, Chen J, Yang S, Zhao M, Xue Y. Transcriptome sequencing analysis of root in soybean responding to Mn poisoning. Int J Mol Sci. 2023;24(16):12727.
34. Rasmussen JA, Villumsen KR, Ernst M, Hansen M, Forberg T, Gopalakrishnan S, Gilbert MT, Bojesen AM, Kristiansen K, Limborg MT. A multi-omics approach unravels metagenomic and metabolic alterations of a probiotic and synbiotic additive in rainbow trout (*Oncorhynchus mykiss*). Microbiome. 2022;10(1):21.
35. Navarro-Reig M, Jaumot J, García-Reiriz A, Tauler R. Evaluation of changes induced in rice metabolome by cd and Cu exposure using LC-MS with XCMS and MCR-ALS data analysis strategies. Anal Bioanal Chem. 2015;407:8835–47.
36. Kieffer DA, Piccolo BD, Vaziri ND, Liu S, Lau WL, Khazaeli M, Nazertehrani S, Moore ME, Marco ML, Martin RJ, Adams SH. Resistant starch alters gut Microbiome and metabolomic profiles concurrent with amelioration of chronic kidney disease in rats. Am J Physiol Ren Physiol. 2016;310(9):F857–71.
37. Xue Y, Zhuang Q, Zhu S, Xiao B, Liang C, Liao H, Tian J. Genome wide transcriptome analysis reveals complex regulatory mechanisms underlying phosphate homeostasis in soybean nodules. Int J Mol Sci. 2018;19(10):2924.
38. Zhuang Q, Xue Y, Yao Z, Zhu S, Liang C, Liao H, Tian J. Phosphate starvation responsive GmSPX5 mediates nodule growth through interaction with GmNF-YC4 in soybean (*Glycine max*). Plant J. 2021;108(5):1422–38.
39. Li G, Song H, Li B, Kronzucker HJ, Shi W. Auxin resistant1 and PIN-FORMED2 protect lateral root formation in Arabidopsis under iron stress. Plant Physiol. 2015;169(4):2608–23.
40. Liu L, Si L, Zhang L, Guo R, Wang R, Dong H, Guo C. Metabolomics and transcriptomics analysis revealed the response mechanism of alfalfa to combined cold and saline-alkali stress. Plant J. 2024;119(4):1900–19.
41. Gu Y, Fan X, Jiang K, Liu P, Chang H, Andom O, Cheng J, Li Z. Omics analysis of 'shine Muscat'grape grafted on different rootstocks in response to cadmium stress. Sci Total Environ. 2024;936:173472.

42. Shen C, Huang YY, Xin JL, He CT, Yang ZY. A novel MicroRNA lamiR-4-3p from water spinach (*Ipomoea aquatica* Forsk.) increased cd uptake and translocation in *Arabidopsis Thaliana*. Environ Sci Pollut Res. 2022;29(27):41375–85.
43. Riaz M, Yan L, Wu X, Hussain S, Aziz O, Jiang C. Boron supply maintains efficient antioxidant system, cell wall components and reduces aluminum concentration in roots of trifoliate orange. Plant Physiol Biochem. 2019;137:93–101.
44. Medda S, Dessena L, Mulas M. Monitoring of the PAL enzymatic activity and polyphenolic compounds in leaves and fruits of two Myrtle cultivars during maturation. Agriculture. 2020;10(9):389.
45. Gao MY, Chen XW, Huang WX, Wu L, Yu ZS, Xiang L, Mo CH, Li YW, Cai QY, Wong MH, Li H. Cell wall modification induced by an arbuscular mycorrhizal fungus enhanced cadmium fixation in rice root. J Hazard Mater. 2021;416:125894.
46. Pawlak-Sprada S, Arasimowicz-Jelonek M, Podgórska M, Deckert J. Activation of phenylpropanoid pathway in legume plants exposed to heavy metals. Part I. Effects of cadmium and lead on phenylalanine ammonia-lyase gene expression, enzyme activity and lignin content. Acta Biochim Pol. 2011;58(2):211–6.
47. Yang X, Kang Y, Liu Y, Shi M, Zhang W, Fan Y, Yao Y, Li H, Qin S. Integrated analysis of miRNA-mRNA regulatory networks of potato (*Solanum tuberosum* L.) in response to cadmium stress. Ecotoxicol Environ Saf. 2021;224:112682.
48. Ribeiro C, de Marcos Lapaz A, de Freitas-Silva L, Ribeiro KV, Yoshida CH, Dal-Bianco M, Cambraia J. Aluminum promotes changes in rice root structure and ascorbate and glutathione metabolism. Physiol Mol Biol Plants. 2022;28(11):2085–98.
49. Yang W, Feng H, Zhou J, Jia T, Tang T, Zhang H, Peng Y. Exogenous silicon induces aluminum tolerance in white clover (*Trifolium repens*) by reducing aluminum uptake and enhancing organic acid secretion. PeerJ. 2024;12:e17472.
50. Mohanty S, Das AB, Das P, Mohanty P. Effect of a low dose of aluminum on mitotic and meiotic activity, 4 C DNA content, and pollen sterility in rice, *Oryza sativa* L. cv. Lalat Ecotoxicol Environ Saf. 2004;59(1):70–5.
51. Sun H, Qian Q, Wu K, Luo J, Wang S, Zhang C, Ma Y, Liu Q, Huang X, Yuan Q, Han R. Heterotrimeric G proteins regulate nitrogen-use efficiency in rice. Nat Genet. 2014;46(6):652–6.
52. Yang LT, Hu NJ, Fu QX, Chen XY, Ren YM, Ye X, Lai NW, Chen LS. Effects of aluminum (Al) stress on nitrogen (N) metabolism of leaves and roots in two citrus species with different al tolerance. Sci Hortic. 2024;334:113331.
53. Zhao XQ, Guo SW, Shinmachi F, Sunairi M, Noguchi A, Hasegawa I, Shen RF. Aluminium tolerance in rice is antagonistic with nitrate preference and synergistic with ammonium preference. Ann Bot. 2013;111(1):69–77.
54. Qu X, Zhou J, Masabni J, Yuan J. Phosphorus relieves aluminum toxicity in oil tea seedlings by regulating the metabolic profiling in the roots. Plant Physiol Biochem. 2020;152:12–22.
55. Liu Y, Tao J, Cao J, Zeng Y, Li X, Ma J, Huang Z, Jiang M, Sun L. The beneficial effects of aluminum on the plant growth in *Camellia Japonica*. J Soil Sci Plant Nutr. 2020;20:1799–809.
56. Lin Q, Fan M, Peng X, Ma J, Zhang Y, Yu F, Wu Z, Liu B. Response of *Vallisneria natans* to aluminum phytotoxicity and their synergistic effect on nitrogen, phosphorus change in sediments. J Hazard Mater. 2020;400:123167.
57. Loomis WD, Durst RW. (1992). Chemistry and biology of boron. BioFactors (Oxford, England). 1992;3(4):229–239.
58. O'Neill MA, Eberhard S, Albersheim P, Darvill AG. Requirement of Borate cross-linking of cell wall rhamnogalacturonan II for Arabidopsis growth. Science. 2001;294(5543):846–9.
59. Fleischer A, O'Neill MA, Ehwald R. The pore size of non-graminaceous plant cell walls is rapidly decreased by Borate ester cross-linking of the pectic polysaccharide rhamnogalacturonan II. Plant Physiol. 1999;121(3):829–38.
60. Hayashi KI, Arai K, Aoi Y, Tanaka Y, Hira H, Guo R, Hu Y, Ge C, Zhao Y, Kasahara H, Fukui K. The main oxidative inactivation pathway of the plant hormone auxin. Nat Commun. 2021;12(1):6752.
61. Ranjan A, Sinha R, Lal SK, Bishi SK, Singh AK. Phytohormone signalling and cross-talk to alleviate aluminium toxicity in plants. Plant Cell Rep. 2021;40(8):1331–43.
62. de Figueiredo MR, Strader LC. Intrinsic and extrinsic regulators of Aux/IAA protein degradation dynamics. Trends Biochem Sci. 2022;47(10):865–74.
63. Hu J, Su H, Cao H, Wei H, Fu X, Jiang X, Song Q, He X, Xu C, Luo K. AUXIN RESPONSE FACTOR7 integrates Gibberellin and auxin signaling via interactions between DELLA and AUX/IAA proteins to regulate cambial activity in Poplar. Plant Cell. 2022;34(7):2688–707.
64. Ahmad P, Abass Ahanger M, Nasser Alyemeni M, Wijaya L, Alam P, Ashraf M. Mitigation of sodium chloride toxicity in *Solanum lycopersicum* L. by supplementation of jasmonic acid and nitric oxide. J Plant Interact. 2018;13(1):64–72.
65. Luo H, He W, Li D, Bao Y, Riaz A, Xiao Y, Song J, Liu C. Effect of Methyl jasmonate on carotenoids biosynthesis in germinated maize kernels. Food Chem. 2020;307:125525.
66. Wang F, Wan C, Wu W, Pan Y, Cheng X, Li C, Pi J, Chen X. Exogenous Methyl jasmonate (MeJA) enhances the tolerance to cadmium (Cd) stress of Okra (*Abelmoschus esculentus* L.) plants. Plant Cell Tissue Organ Cult. 2023;155(3):907–22.
67. Ramabulana AT, Steenkamp PA, Madala NE, Dubery IA. Profiling of altered metabolomic States in *Bidens Pilosa* leaves in response to treatment by Methyl jasmonate and Methyl salicylate. Plants. 2020;9(10):1275.
68. Thu HP, Thu TN, Thao ND, Le Minh K, Do Tan K. Evaluate the effects of salt stress on physico-chemical characteristics in the germination of rice (*Oryza sativa* L.) in response to Methyl salicylate (MeSA). Biocatal Agric Biotechnol. 2020;23:101470.
69. He G, Yang P, Tang Y, Cao Y, Qi X, Xu L, Ming J. Mechanism of exogenous cytokinins inducing bulbil formation in *Lilium lancifolium* in vitro. Plant Cell Rep. 2020;39:861–72.
70. Fathy M, Saad Eldin SM, Naseem M, Dandekar T, Othman EM, Cytokinins. Wide-spread signaling hormones from plants to humans with high medical potential. Nutrients. 2022;14(7):1495.
71. Tian J, Ma Y, Chen Y, Chen X, Wei A. Plant hormone response to low-temperature stress in cold-tolerant and cold-sensitive varieties of *Zanthoxylum bungeanum* Maxim. Front. Plant Sci. 2022;13:847202.
72. Wu BS, Chen XF, Rao RY, Hua D, Huang WL, Chen WS, Yang LT, Huang ZR, Ye X, Wu J, Chen LS. Both hormones and energy-rich compounds play a role in the mitigation of elevated pH on aluminum toxicity in *Citrus sinensis* leaves. Ecotoxicol Environ Saf. 2024;283:116975.
73. Zhang P, Liu F, Abdelrahman M, Song Q, Wu F, Li R, Wu M, Herrera-Estrella L, Tran LS, Xu J. ARR1 and ARR12 modulate arsenite toxicity responses in *Arabidopsis* roots by transcriptionally controlling the actions of *NIP1; 1* and *NIP6; 1*. Plant J. 2024;120(4):1536–51.
74. Savchenko T, Walley JW, Chehab EW, Xiao Y, Kaspi R, Pye MF, Mohamed ME, Lazarus CM, Bostock RM, Dehesh K. Arachidonic acid: an evolutionarily conserved signaling molecule modulates plant stress signaling networks. Plant Cell. 2010;22(10):3193–205.
75. Ibarra AA, Wrobel K, Barrientos EY, Escobosa AR, Corona JF, Donis IE, Wrobel K. Impact of cr (VI) on the oxidation of polyunsaturated fatty acids in *Helianthus annuus* roots studied by metabolomic tools. Chemosphere. 2019;220:442–51.
76. Hu C, Shi J, Quan S, Cui B, Kleessen S, Nikoloski Z, Tohge T, Alexander D, Guo L, Lin H, Wang J. Metabolic variation between Japonica and indica rice cultivars as revealed by non-targeted metabolomics. Sci Rep. 2014;4(1):5067.
77. Yu J, Tang L, Qiao F, Liu J, Li X. Physiological and transcriptomic analyses reveal the mechanisms underlying Methyl jasmonate-induced mannitol stress resistance in banana. Plants. 2024;13(5):712.
78. Li C, Yao Y, Liu X, Chen H, Li X, Zhao M, Zhao H, Wang Y, Cheng Z, Wang L, Cheng J. Integrated metabolomics, transcriptomics, and proteomics analyses reveal co-exposure effects of polycyclic aromatic hydrocarbons and cadmium on ryegrass (*Lolium Perenne* L.). Environ. Int. 2023;178:108105.
79. Shaikh SR, Edidin M. Polyunsaturated fatty acids, membrane organization, T cells, and antigen presentation. Am J Clin Nutr. 2006;84(6):1277–89.
80. Mano J. Reactive carbonyl species: their production from lipid peroxides, action in environmental stress, and the detoxification mechanism. Plant Physiol Biochem. 2012;59:90–7.
81. Takagi D, Ifuku K, Ikeda KI, Inoue KI, Park P, Tamoi M, Inoue H, Sakamoto K, Saito R, Miyake C. Suppression of chloroplastic alkenal/one oxidoreductase represses the carbon catabolic pathway in Arabidopsis leaves during night. Plant Physiol. 2016;170(4):2024–39.
82. Parvez S, Long MJ, Poganik JR, Aye Y. Redox signaling by reactive electrophiles and oxidants. Chem Rev. 2018;118(18):8798–888.
83. Saxena A, Sonowal H, Ramana KV. Transcriptional factor modulation by lipid peroxidation-derived aldehydes. Mol Nutr Fats Acad Press, 2019: 419–31.

Publisher's note